Biosensors and Bioelectronics 28 (2011) 386–392

Contents lists available at ScienceDirect

Biosensors and Bioelectronics

journal homepage: www.elsevier.com/locate/bios

Polymer based biosensor for rapid electrochemical detection of virus infection of human cells

Katrine Kiilerich-Pedersen[a], Claus R. Poulsen[a], Titoo Jain[b], Noemi Rozlosnik[a,*]

[a] Technical University of Denmark, Department of Micro- and Nanotechnology, Oersteds Plads 345 East, DK-2800 Kongens Lyngby, Denmark
[b] University of Copenhagen, Nano-Science Center and Department of Chemistry, Universitetsparken 5, DK-2100 Copenhagen, Denmark

ARTICLE INFO

Article history:
Received 11 May 2011
Received in revised form 18 July 2011
Accepted 21 July 2011
Available online 28 July 2011

Keywords:
Conductive polymer
PEDOT:TsO
Electrochemical impedance spectroscopy (EIS)
Human cytomegalovirus (CMV)
Human fibroblast cells
Atomic force microscopy (AFM)
Scanning ion conductance microscopy (SICM)

ABSTRACT

The demand in the field of medical diagnostics for simple, cost efficient and disposable devices is growing. Here, we present a label free, all-polymer electrochemical biosensor for detection of acute viral disease. The dynamics of a viral infection in human cell culture was investigated in a micro fluidic system on conductive polymer PEDOT:TsO microelectrodes by electrochemical impedance spectroscopy and video time lapse microscopy.

Employing this sensitive, real time electrochemical technique, we could measure the immediate cell response to cytomegalovirus, and detect an infection within 3 h, which is several hours before the cytopathic effect is apparent with conventional imaging techniques. Atomic force microscopy and scanning ion conductance microscopy imaging consolidate the electrochemical measurements by demonstrating early virus induced changes in cell morphology of apparent programmed cell death.

1. Introduction

In a global community, the outbreak of infectious diseases contributes to the fear of severe pandemics, and is a source of worry for the population. In recent years, emerging viruses have been a focus of attention (e.g. Dengue virus, West Nile virus, Influenza A virus) and has thus emphasized the need for new effective tools in medical diagnostics. Conventional diagnostic methods for detection of acute viral disease, such as polymerase chain reactions (PCR) and enzyme linked immunosorbent assays (ELISA) are time consuming, labour intensive and expensive (Cheng et al., 2009; Lazcka et al., 2007). Accordingly, it is important to develop effective point-of-care tools to detect, control and confine the spread of virulent diseases in the near future.

Recently, there has been great advancements in the biosensor technology, and in particular impedimetric sensors have attracted attention for the high sensitivity, reliability and simplicity (Chen et al., 2010; Primiceri et al., 2009; Diouani et al., 2008; Hnaien et al., 2008; Daniels and Pourmand, 2007; Mathebula et al., 2009).

Among cell based assays, electrochemical impedance spectroscopy combined with microelectrode arrays provides a platform for label free detection of the cellular response to different drugs or pathogens (Arias et al., 2010; Ona and Shibata, 2010). The interaction between a cell monolayer and the electrode surface can be monitored in real time by applying a small amplitude alternate-current (AC) electric field. Cells are essentially non conducting at low frequencies and the cell membrane offers a significant barrier to current flow, so that the amplitude of the AC field is an indication of the cell volume or size (Cheung et al., 2005). Average alterations in the three dimensional shape of cells is then computed by integrating over a monolayer of hundreds or thousands of cells. The measured impedance reflects changes in the attachment and morphology of cells, and reaches its maximum when the electrode is completely covered (Giaever and Keese, 1986; Keese and Giaever, 1994).

Electrochemical impedance spectroscopy (EIS) measured on cells cultured on a microelectrode array is very sensitive to small changes in the cell membrane capacitance and resistance. These parameters are good indicators for the well being of cells at a given cell morphology. The real time detection of cell impedance gives an efficient and rapid technique for non invasive monitoring of the response of human cells in culture to the challenge of a virus infection (McCoy and Wang, 2005; Campbell et al., 2007).

* Corresponding author.
E-mail addresses: noemi.rozlosnik@nanotech.dtu.dk, noro58@gmail.com (N. Rozlosnik).

0956-5663/$ – see front matter © 2011 Elsevier B.V. All rights reserved.
doi:10.1016/j.bios.2011.07.053

In general, viral infections can induce degenerative morphological changes in cell cultures; cell detachment from substrate, release of cell–cell adhesions, cell round up and eventually cell death. Beside the morphological effects, these changes in the cells produce a decline in the resistance and an increase in the capacitance in the impedance signal (McCoy and Wang, 2005; Campbell et al., 2007).

Polymer based microfluidic systems meet the requirements of disposable devices, low sample consumption, cost efficiency, reliability, and fast response time, which make the systems ideal for point-of-care analysis. By employing conductive polymers as electrode materials, the additional advantageous properties of inexpensive electrode fabrication and easy electrode functionalization can be achieved (Rozlosnik, 2009). This feature is of great importance in biosensor applications, where particles or cells are immobilized directly on the electrode surface.

In the present study, an all polymer microsystem with a PEDOT:TsO microelectrode array was developed and exploited for real time and label free electrochemical detection of the effect of human cytomegalovirus (CMV) on cells. In this work, we show that the novel biosensor technology demonstrates a fast and sensitive response to the small changes in the cell morphology induced by infectious agents, and thus presents a strongly competitive alternative to the current detection techniques opening a wide range of applications.

2. Experimental procedures

2.1. All polymer microdevice

The all polymer microfluidic device was composed of four layers (Fig. 1). Top and bottom pieces were fabricated from the cyclic olefin copolymer TOPAS 5013L (TOPAS Advanced Polymers, Germany; $T_g \simeq 134\,^{\circ}C$) by injection moulding (Victory 80/45 Tech, Engel, Germany). The top part contained access ports in standard luer lock size for fluid inlets, outlets and electrical connections. The second layer – microchannels and reservoirs – were defined in an 80 μm thick, pressure sensitive adhesive (PSA, ARcare 90106, Adhesive Research, USA) by laser ablation (Duo Lase CO_2 laser, Synrad Inc., USA). The electrodes in the third layer were made from a conductive polymer, poly(3,4-ethylenedioxythiophene) doped with tosylate (PEDOT:TsO). The EDOT monomer (Baytron M) and Fe(III)-tosylate (40% in butanol, Baytron C) were purchased from Bayer AG (Leverkusen, Germany). Conductive polymer coatings were fabricated using in situ polymerization of EDOT with Fe(III) tosylate as oxidation agent. This yields a highly conducting polymer (PEDOT:TsO) coating with a sheet resistance of ~100 Ω/sq (Hansen et al., 2010; Daugaard et al., 2008).

Electrodes and electrical connection patches were patterned in the PEDOT:TsO layer using standard photo lithographic processing techniques in the Danchip Cleanroom (Technical University of Denmark, Denmark).

The final chip was assembled by thermal assisted bonding at 55 °C with 55 kg force applied for 5 min in an in house build, LabView (National Instruments, USA) controlled press. Prior to the bonding step, top and bottom pieces with the patterned PEDOT:TsO electrode layer were cleaned in air plasma (50 W, 30 s; OEM-6AM-1B, ENI Power Systems, USA)

2.2. Cell culture

Human foreskin fibroblast (HFF; ATCC Cat. No. SCRC-1041; LOT: 58592555) cells were cultured in monolayers in a humidified incubator at 37 °C, 5% CO_2 in Dulbecco's modified Eagle's medium (DMEM, Invitrogen, Carlsbad, California, USA) supplemented with 10% Fetal Bovine Serum (FBS, F7524, Sigma, St. Louis, Missouri, USA), Penicillin 10,000 U/ml, and Streptomycin 10,000 μg/ml (PS, DE17-602E, Lonza, Basel, Switzerland). The cells were subcultured by trypsination for maintenance every third day, or at ~80–90% confluence.

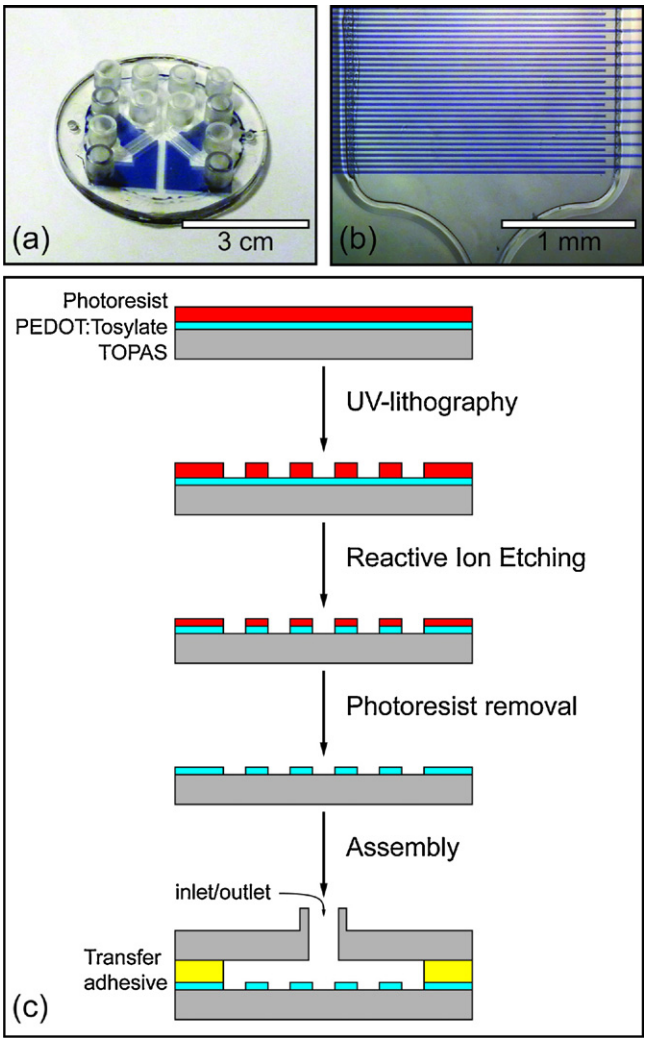

Fig. 1. Microdevice production: (a) Microdevice with two functional channels fabricated in TOPAS (uncolored) and PEDOT:TsO (blue), (b) microchannel with interdigitated microelectrode array, and (c) schematic representation of fabrication steps. (For interpretation of the references to color in this figure legend, the reader is referred to the web version of the article.)

2.3. Preparation of virus stock

Human CMV, (Towne strain; kindly provided by Thomas Kledal, Inagen ApS, Denmark) was employed as infectious agent against HFF cells. Human CMV is a ubiquitous β-herpesvirus that causes widespread, persistent infection in the human host. Virus was propagated and titered in HFFs, and infection of cells was performed in DMEM supplemented with 10% Nu Serum (355500, BD Biosciences), and 1% PS. Virus with a multiplicity of infection (MOI) of 0.01 was adsorbed for 2 h at 37 °C, overlaid with medium, and incubated for the required number of hours post infection (hpi). The cell medium was changed at 100% cytopathic effect, and virus was harvested two days later.

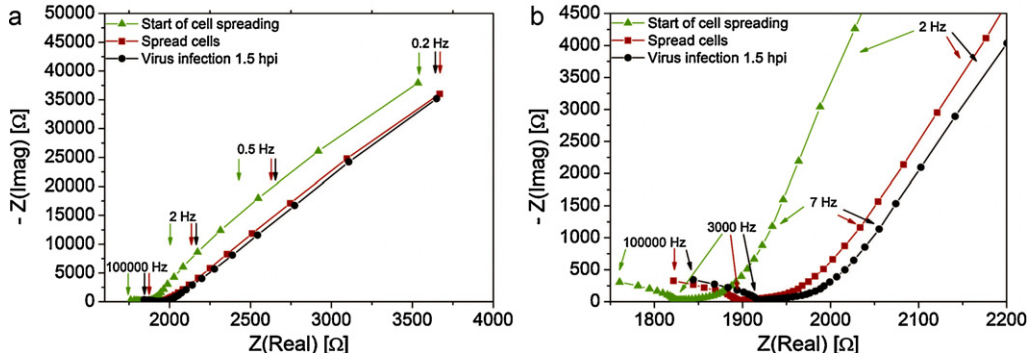

Fig. 2. EIS spectra of the impedimetric sensor presented in Nyquist plots. (a) The full recoded range, and (b) zoom in higher frequency regime. The green, red and black traces refer to (i) immediately before cells were seeded in the microchip, (ii) 14 h after cells seeding, and (iii) cells infected with human CMV, respectively. (For interpretation of the references to color in this figure legend, the reader is referred to the web version of the article.)

2.4. Virus purification

Medium from infected cell cultures was collected and centrifuged at 1260 × *g* for 10 min at 4 °C, and the virus was sedimented by centrifugation at 24, 336 × *g* for 1 h at 4 °C. The pelleted virus was resuspended in DMEM supplemented with 1% PS, layered over 20% sorbitol in Tris-buffered saline, and purified by centrifugation at 50, 228 × *g* over night at 4 °C. The pelleted virus was resuspended in DMEM supplemented with 1% PS, aliquoted, and stored at −80 °C. Virus titer was determined by plaque titration assay using methyl cellulose and crystal violet staining.

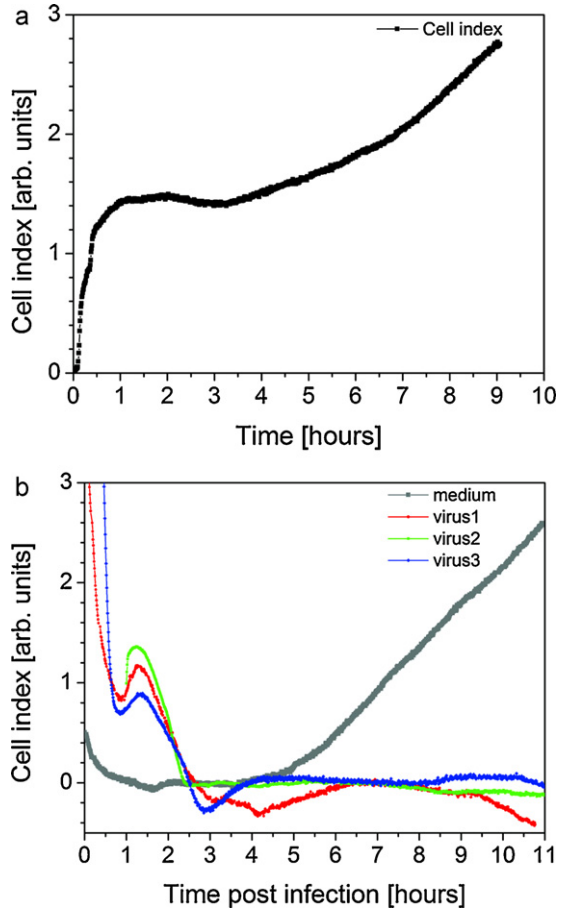

Fig. 3. Electrochemical detection of cell spreading and proliferation (a) and the effect of human CMV infection (b) on HFF cells cultured on PEDOT:TsO microelectrodes in the biosensor. The cell index – defined in Eq. (1) – was measured at a frequency of 2 Hz. The green, red and blue traces refer to three independent measurements on cells infected with human CMV at a MOI of 3 at $t = 0$. The grey trace refers to the measurement adding cell medium instead of virus containing solution at $t = 0$. (For interpretation of the references to color in this figure legend, the reader is referred to the web version of the article.)

2.5. EIS on cell culture

Healthy HFFs were seeded directly on a conductive polymer electrode surface in the micro channel of the chip (Fig. 1), and allowed to attach and spread on the substrate and acclimatize over night. EIS was used to monitor the electrical properties of the cell monolayer before and after the introduction of pathogen. The microchip was placed in a temperature controlled incubation chamber, and EIS experimentation (no redox couple added) was carried out in a tightly controlled environment at 37 °C.

Impedance spectra were recorded every 33 s in the frequency range from 0.2 Hz to 100 KHz with an amplitude of 10 mV in a two-electrode setup.

The optimal frequency for the time dependent analysis – determined by the highest response to changes on the cells – was found at 2 Hz (Fig. 2). This frequency was used for all analyses. We defined a cell index

$$\mathrm{CI} = (Z_{\mathrm{cell}}(t)Z_{\mathrm{cell}}(0) - 1) \cdot 100 \quad (1)$$

where $Z_{\mathrm{cell}}(0)$ and $Z_{\mathrm{cell}}(t)$ are the measured impedance on the chip at the beginning of the measurement and after a time t, respectively.

The cytopathic effect on cells was monitored in an inverted phase contrast microscope (Nikon Eclipse Ti-S/L100, Japan) with auto focusing controlled by dedicated software. A digital camera (VisiCam 3000, VWR) recorded time lapse movies with intervals of 15 min for 20 h. In the presented results, cells were inoculated with human CMV at an MOI of 3.

2.6. Imaging virus infected cells

HFFs were grown in petri dishes and infected with human CMV at a MOI of 5 in 1 ml. At given time points post infection (.5, 1, 1.5, 2, and 3 h), cells were washed twice with preheated infection medium to remove residual virus, fixed in 2% glutaraldehyde in Phosphate Buffered Saline (PBS; (1×), Lonza) for 60 min at room temperature, and washed with PBS for 15 min at 4 °C. Samples for investigations by scanning ion conductance microscopy (SICM) were stored in PBS at 4 °C. Fixed cell samples for atomic force microscopy (AFM) studies were dehydrated by increasing concentrations of ethanol (30–99%) for 3 min on a shaker at room temperature and freeze dried over night (Tojima et al., 1998; Kirk et al., 2009).

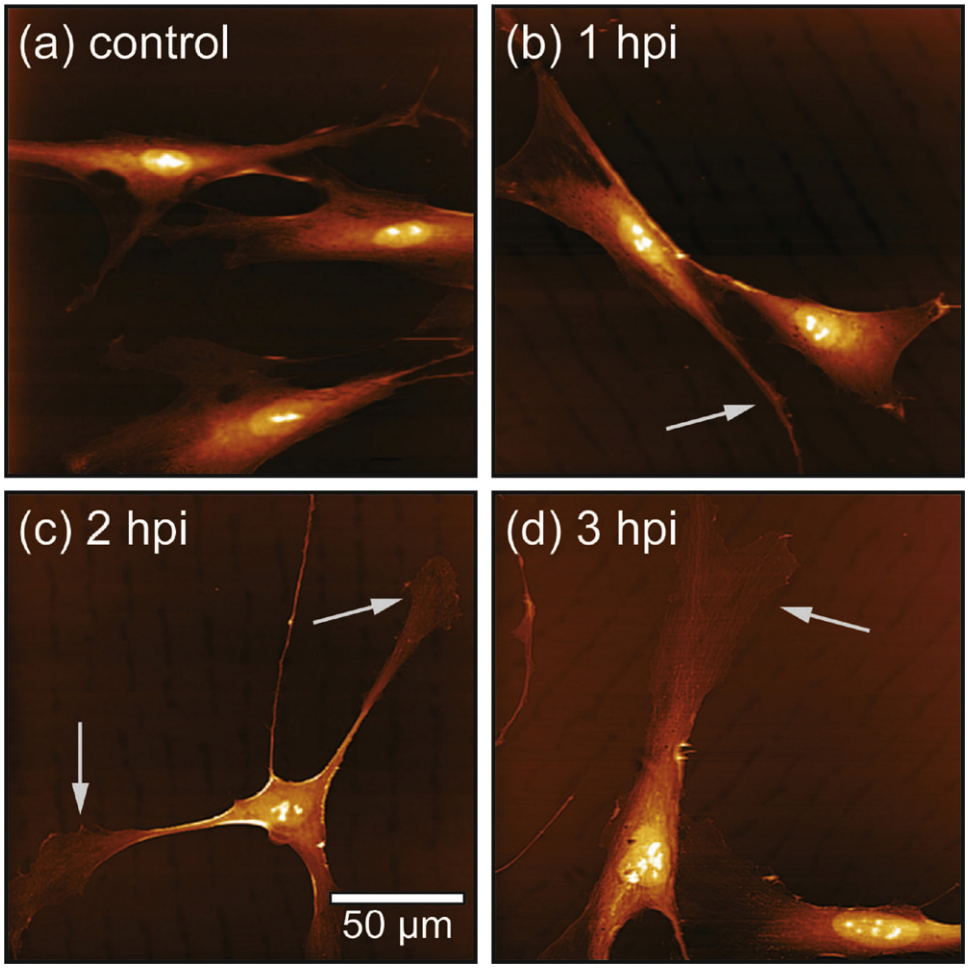

Fig. 4. AFM topography images of fixed HFF cells at different time points post infection with human CMV. Cell morphology was affected by virus, and arrows indicate some adverse cellular protrusions. (a) Control cell. (b) 1 hpi the cell has contracted and formed narrow filamentous projections. (c) 2 hpi the filamentous projections are beginning to spread-out. (d) 3 hpi the cell body has somewhat recovered its size and shape though adverse spread-out protrusions remain present. Enlargment of the nucleus and nuclear DNA fragmentation can be observed, which are the hallmarks of apoptosis.

2.7. AFM imaging

AFM images were recorded with a DME-SPM (Dualscope II, Denmark) in tapping mode using standard non contact high frequency cantilevers (TAP300Al, Budget Sensors) with a force constant of 40 N/m. AFM examinations were carried out in air at room temperature.

2.8. SICM imaging

SICM images were recorded with an XE-Bio system (Park Systems, Korea) in adaptive Approach-Retract-Scan (ARS) mode with borosilicate capillary glass pipettes (inner diameter of 80 nm). SICM examinations were carried out in PBS at room temperature.

3. Results and discussion

An all polymer microsystem was fabricated by injection moulding and standard photo lithographic processing techniques (Fig. 1), and exploited for label free, real time, electrochemical detection of infectious agents in human cell culture.

3.1. Microchip design considerations

The low cost microsystem was fabricated in TOPAS with interdigitated electrodes in the conductive polymer PEDOT:TsO. PEDOT was selected for its high environmental stability, biocompatibility, transparency to visible light and ease of processing (Rozlosnik, 2009). Before producing the all polymer microdevice, finite element method simulations (COMSOL Multiphysics 3.5) were made for optimizing the geometry of the conductive polymer electrodes and the microchannel shape (results are not shown). Microchannels offer refined fluid control, low sample consumption, and reduced interference, which is favorable in many biological and medical applications (Stott et al., 2010).

Although PEDOT:TsO is a redox system, this impedimetric sensor is based on the low frequency response (i.e. non faradaic region) with no additional electron-transfer mediators. Previous studies on impedimetric immunosensors have shown that this scheme is more amenable to biosensor applications (Berggren et al., 2001; Rickert et al., 1996), because the long term presence of a redox-couple reduces the activity of the enzymes (Rickert et al., 1996).

The biocompatibility of the all polymer biosensor chip was evaluated by culturing HFF cells in the chip for a week (see Fig. S1 in Supplemental Data available online). The cells adhered and proliferated normally on TOPAS and PEDOT:TsO, and no significant change in the morphology of cells could be observed during this period. On the other hand, the morphological changes on the virus infected cell culture could easily be observed on the samples in a time frame of 12–24 hpi (see Fig. S2 in Supplemental Data available online).

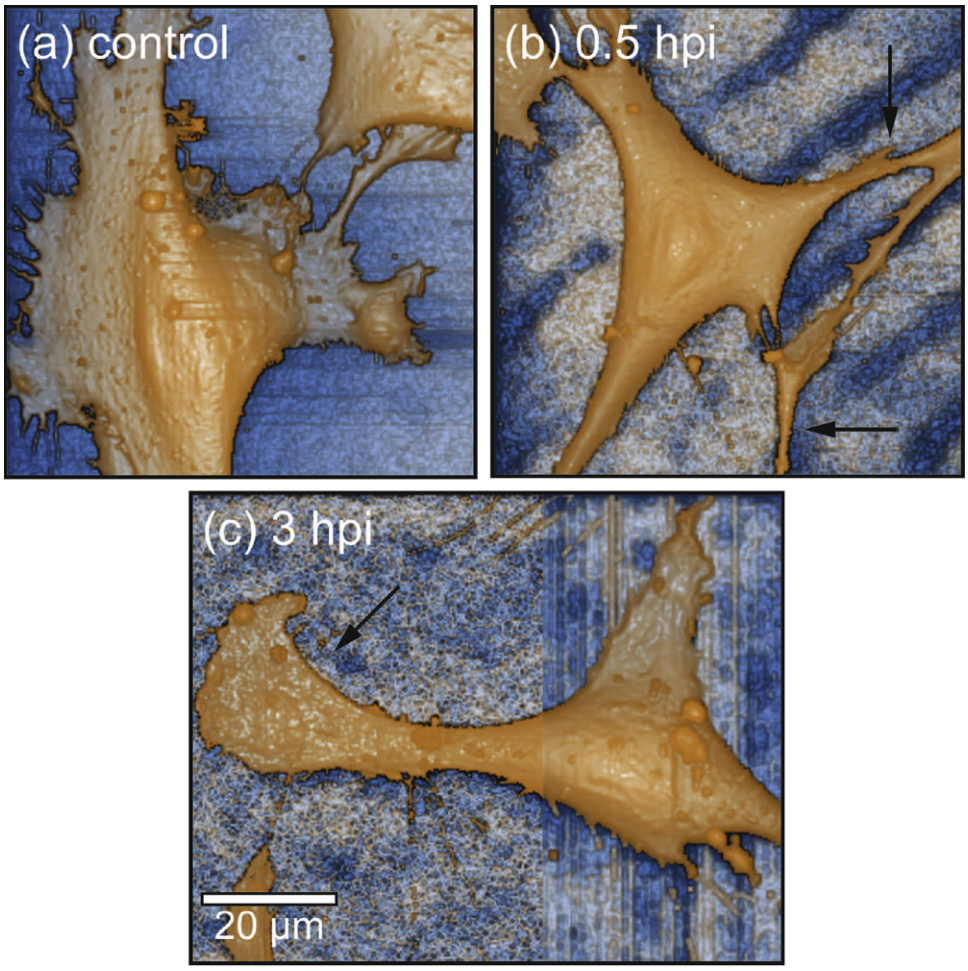

Fig. 5. SICM topography images of fixed HFF cells at different time points post infection with human CMV. Cell morphology was affected by virus, and arrows indicate some adverse cellular protrusions.(a) Control cell. (b) 30 min post infection the cell has contracted and formed narrow filamentous projections. (c) 3 hpi the cell body has recovered its size and shape though adverse spread-out protrusions remain present.

3.2. Electrochemical detection of virus

HFF cells were cultured in a monolayer on the conductive polymer substrate over night to allow the cells to get acclimatized before virus inoculation.

Fig. 2 shows the EIS spectra of the impedimetric sensor presented in Nyquist plots. The three traces refer to (i) immediately before cells were seeded in the microchip, (ii) 14 h after cells seeding, and (iii) cells infected with human CMV, respectively. The higher frequency regime (>3 kHz, semicircle) corresponds to the charge transfer at the electrode-solution interface (faradaic current) and is determined by the charge transfer resistance and the double layer capacitance, while the impedance at low frequencies is dominated by diffusion (i.e. mass transport of ions). Considering that the ion diffusion is expected to be much faster in the liquid solution than in a solid material, this part of the spectrum is anticipated to be the most sensitive for the changes on the electrode surface. At very low frequencies the measurement of one single point takes relatively long time, and the sensitivity is not improved significantly, therefore we have selected the highest reasonable frequency (i.e. 2 Hz).

The initial attachment and spreading of cells on the electrode surface was reflected by a gradual increase in the impedance until a plateau was reached (Fig. 3a), because the healthy cells act as an insulating layer on the electrode surface (Giaever and Keese, 1986) by blocking the diffusion of the ions to the electrodes. A second rise in the cell index is observed after 4 h, reflecting the proliferation of cells (Fig. 3a).

When the cells were infected with human CMV at a MOI of 3 at $t = 0$, the infection was detectable within 2 hpi – several hours before the cytopathic effect appeared. The immediate cell response to virus was mirrored by a drastic fluctuation in the impedance at low frequencies, and thus in the cell index (Fig. 3b). At 2 Hz, the absolute impedance peaked at around 1.5 hpi to reach a local maximum and then gradually decreased to a local minimum in the hours that followed, reflecting the inter- and intra-remodeling events caused by the virus. No sign of proliferation was observed on virus infected cells.

In control measurements, cell medium was added at $t = 0$ instead of virus containing medium. The absolute impedance decreased slightly to reach a plateau within 30 min after the physical manipulation. Over a period of 10 h, the absolute impedance increased in response to proliferation (Fig. 3b, grey trace).

In all cases, we observed a linear increase in the impedance signal (a drift) at all frequencies in the system. This drift arose most probably from swelling of the pressure sensitive adhesive, in which the microchannels were defined, and it was subtracted (as a base line) from each impedance curve.

To investigate the effect of the infection in microscopy, high resolution images of healthy and virus infected HFF cells were captured 1, 3 and 8 hpi with human CMV at high dose (MOI 10).

The early cellular changes were not observable in microscope (see Fig. S3 in Supplemental Data available online).

Video time lapse microscopy studies of cell cultures showed that the cytopathic effect of the virus manifested itself approximately 8–10 hpi depending on the MOI (see Virus-infected-cells.mp4 video file in Supplemental Data available online).

The application of EIS as a sensing tool for quantifying virus or drug induced cell death in cell cultures has previously been reported, e.g. cells infected with influenza A virus (McCoy and Wang, 2005), infectious pancreatic necrosis virus (Campbell et al., 2007) or infectious hematopoeitic necrosis virus (Campbell et al., 2007). In those studies, the terminal stages of cell death (lysis and detachment from substrate) were detected by EIS, rather than the early morphological features related to a virus infection. These changes are only detectable after many hours or even days, and they can also be imaged by phase contrast microcopy. In certain cases a clear spike in resistance was reported at the time of virus inoculation (McCoy and Wang, 2005; Campbell et al., 2007), however, we presume that this was attributed to physical manipulation and was not caused by the virus. In our measurements, the short term response to virus was directly monitored by the impedance changes, which allowed us to recognise the virus infection in the very early stage (Kukura et al., 2009; Seisenberger et al., 2001).

Cell survival and appearance of the cytopathic effect depend on the dilution of virus. Our preliminary impedimetric studies on cells infected with different dilutions of human CMV indicated that the change in the absolute impedance at 2 Hz was highly dependent on the amount of virus (data not shown). Our data implied that the initial peak shifted in time in response to virus dose. Further investigations are required to determine the exact concentration dependence.

3.3. Early morphological signs of apoptosis

Complementary imaging investigations were performed to understand the biology that gave rise to the drastic changes in impedance associated with virus infection.

AFM of fixed infected cells permit structural investigations of the cell surface at high resolution. Topography scans 1, 2, and 3 hpi (Fig. 4) demonstrate that the cytoskeleton organization is aberrantly rearranged within few hours post infection. During the initial phase of high dose infection (MOI of 5), the cells contract and filamentous projections occur, presumably in response to a calcium influx (Albrecht et al., 1983; Sharon-Friling et al., 2006). Around 3 hpi, the cell body recovers its size and shape, though adverse protrusions remain present. These distinct morphological features – in particular the changes in cell surface area – clarify the impedimetric changes caused by the virus infection.

The topography scans further indicate adverse nuclear morphology, which is a hallmark of apoptosis (Ghibelli et al., 1995; Gadaleta et al., 2002; Jurak et al., 2008). Some viruses have been reported to induce programmed cell death in the absence of viral replication, for instance triggered by the interaction with a cellular membrane receptor or entry and uncoating of the virion (Jan and Griffin, 1999).

AFM images were captured in air to obtain a high resolution, even though the drying process of the samples could influence the 3D cellular structure. Therefore, SICM images were captured in liquid to preserve the cellular structure.

SICM is an emerging non contact scanning tool based on ion currents through a micro pipette, providing true topography of soft samples (Boecker et al., 2007; Korchev et al., 1997). The technique has several advantages over AFM; an essential feature is that no imaging force is exerted on the sample. SICM images (Fig. 5) exhibit detailed information from the cell surface structure, and display fine structures, which are smeared out or not visible in the AFM image. Further, cell–cell interactions are more evident by SICM imaging than AFM imaging. Protrusions and cellular extensions are challenging to sight in the AFM image, however, the cytoskeleton is very detailed, an attribute to the direct mechanical contact during scanning (Rheinlaender et al., 2011). Therefore, the scans obtained by AFM and SICM imaging accentuate different morphological characteristics and thus complement each other.

4. Conclusion

In summary, we have developed a disposable polymer microsystem with PEDOT:TsO microelectrodes for rapid, label free, and real time electrochemical detection of infectious agents in human cell culture. We have demonstrated that an infection of HFF cells with human CMV causes drastic changes in the cell index within the first 3 hpi. Thus, the infection is detectable much faster than by conventional assays. To comprehend the cellular changes at this early stage in the infectious cycle, virus infected cells were examined by AFM and SICM imaging. Our investigations indicated the rearrangement of cytoskeleton organization and the early signs of apoptotic nuclei within 3 h post virus infection explaining the results of the impedance measurements. Compared to conventional inspection techniques, the use of inexpensive electrochemical biosensors (which is also suitable for mass production) can thus significantly reduce the time frame of virus diagnostics.

Acknowledgments

This work was supported by the Danish Research Council for Technology and Production Sciences and the Technical University of Denmark. The authors greatly acknowledge the technical assistance from Brian Choi and Anika Gruetzner in SICM imaging, and Park Systems Corp. and the Europe Demo. Lab. Center for providing the instrument to conduct the SICM research.

Appendix A. Supplementary Data

Supplementary data associated with this article can be found, in the online version, at doi:10.1016/j.bios.2011.07.053.

References

Albrecht, T., Speelman, D., Steinsland, O., 1983. Life Sciences 32, 2273–2278.
Arias, L.R., Perry, C.A., Yang, L., 2010. Biosensors & Bioelectronics 25, 2225–2231.
Berggren, C., Bjarnason, B., Johansson, G., 2001. Electroanalysis 13, 173–180.
Boecker, M., Anczykowski, B., Wegener, J., Schaeffer, T.E., 2007. Nanotechnology 18.
Campbell, C.E., Laane, M.M., Haugarvoll, E., Giaever, I., 2007. Biosensors & Bioelectronics 23, 536–542.
Chen, J., Zhang, J., Yang, H., Fu, F., Chen, G., 2010. Biosensors & Bioelectronics 26, 144–148.
Cheng, X., Chen, G., Rodriguez, W.R., 2009. Analytical and Bioanalytical Chemistry 393, 487–501.
Cheung, K., Gawad, S., Renaud, P., 2005. Cytometry Part A 65A, 124–132.
Daniels, J.S., Pourmand, N., 2007. Electroanalysis 19, 1239–1257.
Daugaard, A.E., Hvilsted, S., Hansen, T.S., Larsen, N.B., 2008. Macromolecules 41, 4321–4327.
Diouani, M.F., Helali, S., Hafaid, I., Hassen, W.M., Snoussi, M.A., Ghram, A., Jaffrezic-Renault, N., Abdelghani, A., 2008. Materials Science & Engineering C: Biomimetic and Supramolecular Systems 28, 580–583.
Gadaleta, P., Vacotto, M., Coulombie, F., 2002. Virus Research 86, 87–92.
Ghibelli, L., Maresca, V., Coppola, S., Gualandi, G., 1995. FEBS Letters 377, 9–14.
Giaever, I., Keese, C.R., 1986. IEEE Transactions on Biomedical Engineering 33, 242–247.
Hansen, T.S., Selmeczi, D., Larsen, N.B., 2010. Journal of Micromechanics and Microengineering 20.
Hnaien, M., Diouani, M.F., Helali, S., Hafaid, I., Hassen, W.M., Renault, N.J., Ghram, A., Abdelghani, A., 2008. Biochemical Engineering Journal 39, 443–449.
Jan, J.T., Griffin, D.E., 1999. Journal of Virology 73, 10296–10302.
Jurak, I., Schumacher, U., Simic, H., Voigt, S., Brunel, W., 2008. Journal of Virology 82, 4812–4822.
Keese, C., Giaever, I., 1994. IEEE Engineering in Medicine and Biology Magazine 13, 402–408.
Kirk, S.E., Skepper, J.N., Donald, A.M., 2009. Journal of Microscopy: Oxford 233, 205–224.

Korchev, Y., Bashford, C., Milovanovic, M., Vodyanoy, I., Lab, M., 1997. Biophysical Journal 73, 653–658.
Kukura, P., Ewers, H., Mueller, C., Renn, A., Helenius, A., Sandoghdar, V., 2009. Nature Methods 6, 923–U85.
Lazcka, O., Del Campo, F.J., Munoz, F.X., 2007. Biosensors & Bioelectronics 22, 1205–1217.
Mathebula, N.S., Pillay, J., Toschi, G., Verschoor, J.A., Ozoemena, K.I., 2009. Chemical Communications, 3345–3347.
McCoy, M.H., Wang, E., 2005. Journal of Virological Methods 130, 157–161.
Ona, T., Shibata, J., 2010. Analytical and Bioanalytical Chemistry 398, 2505–2533.
Primiceri, E., Chiriaco, M.S., Ionescu, R.E., D'Amone, E., Cingolani, R., Rinaldi, R., Maruccio, G., 2009. Microelectronic Engineering 86, 1477–1480.
Rheinlaender, J., Geisse, N.A., Proksch, R., Schaffer, T.E., 2011. Langmuir 27, 697–704.
Rickert, J., Gopel, W., Beck, W., Jung, G., Heiduschka, P., 1996. Biosensors & Bioelectronics 11, 757–768.
Rozlosnik, N., 2009. Analytical and Bioanalytical Chemistry 395, 637–645.
Seisenberger, G., Ried, M., Endress, T., Buning, H., Hallek, M., Brauchle, C., 2001. Science 294, 1929–1932.
Sharon-Friling, R., Goodhouse, J., Colberg-Poley, A.M., Shenk, T., 2006. Proceedings of the National Academy of Sciences of the United States of America 103, 19117–19122.
Stott, S.L., Hsu, C.H., Tsukrov, D.I., Yu, M., Miyamoto, D.T., Waltman, B.A., Rothenberg, S.M., Shah, A.M., Smas, M.E., Korir, G.K., Floyd Jr., F.P., Gilman, A.J., Lord, J.B., Winokur, D., Springer, S., Irimia, D., Nagrath, S., Sequist, L.V., Lee, R.J., Isselbacher, K.J., Maheswaran, S., Haber, D.A., Toner, M., 2010. Proceedings of the National Academy of Sciences of the United States of America 107, 18392–18397.
Tojima, T., Hatakeyama, D., Yamane, Y., Kawabata, K., Ushiki, T., Ogura, S., Abe, K., Ito, E., 1998. Japanese Journal of Applied Physics Part 1: Regular Papers Short Notes & Review Papers 37, 3855–3859.